

The Equation of State of Nuclear Matter from Collective Flows in Intermediate Energy Heavy-Ion Collisions: An Update

Dan Cozma

IFIN-HH
Bucharest, Romania

NUSYM24, 13 September 2024



Overview

Motivation

Model Details

- dcQMD – interaction parametrization
- Threshold effects
- Medium modification of cross-section
- Final state treatment

Study of EoS, Effective Masses, σ^* using Nucleonic Obs

- Framework
- Impact of Different Observables
- Model Dependence
- Constraints

Perspectives

Summary & Conclusions

for details see D.C. arXiv:2407.16411

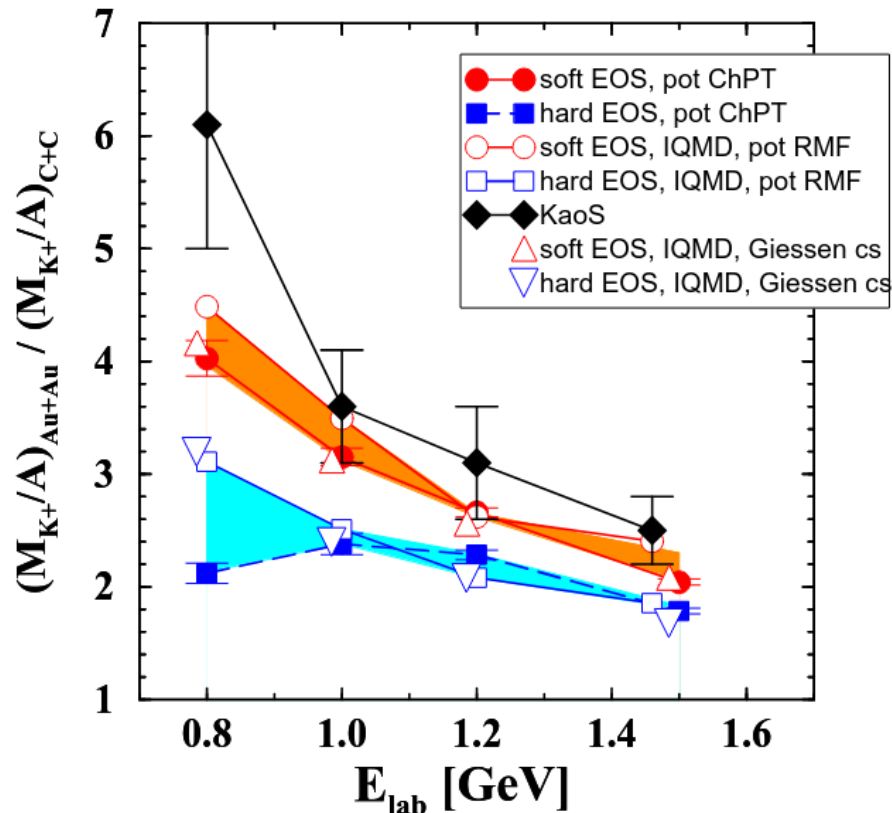
Rare probes in HIC

intermediate energy HIC collisions provide the opportunity to study three different aspects of the in-medium NN interaction:

- in-medium cross-sections
- momentum dependence of optical potential
- density dependence of EoS of cold nuclear matter

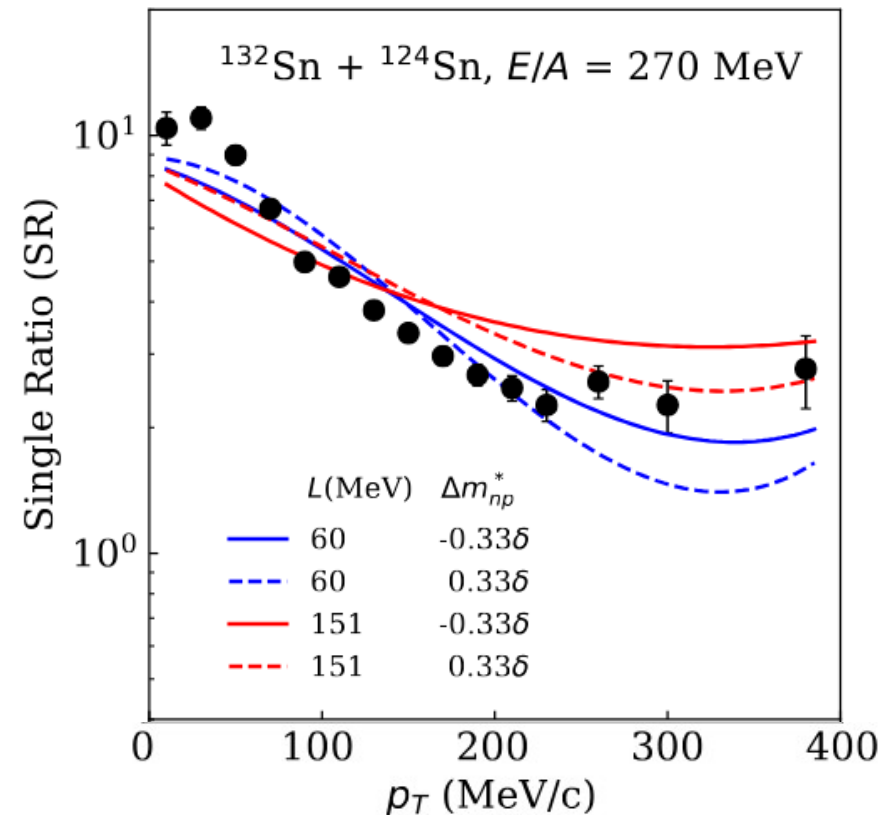
a divide-and-conquer approach has been often employed

K⁺ ratio (KaOS Coll): EoS of SNM



C. Fuchs, PPNP 56, 1 (2006)

π^-/π^+ ratio (S π RIT Coll): symmetry energy



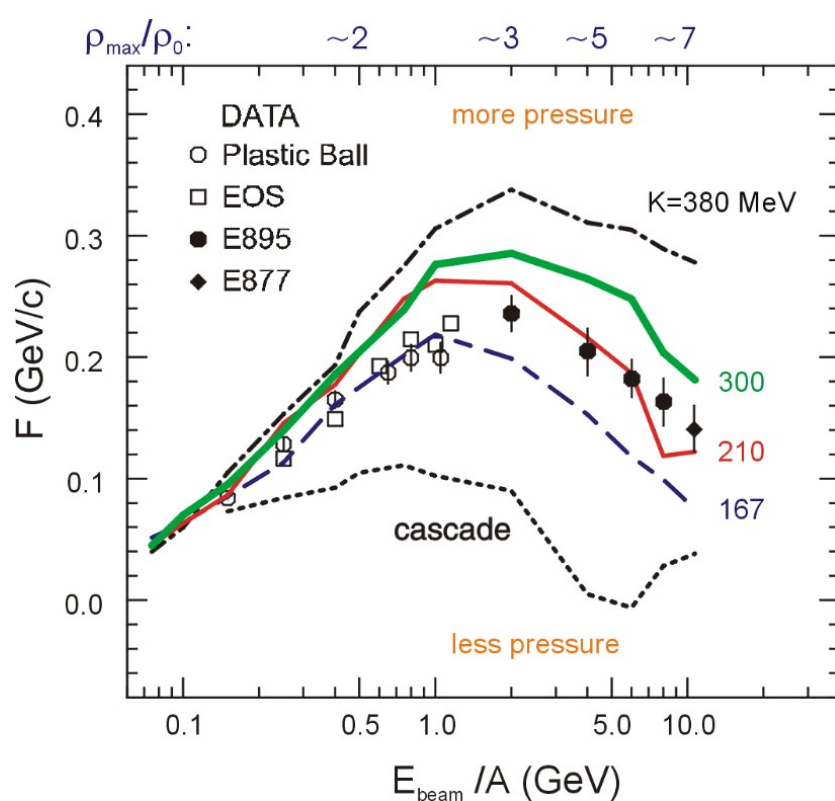
J. Estee et al. PRL 126, 162701 (2021)

Nucleonic Observables

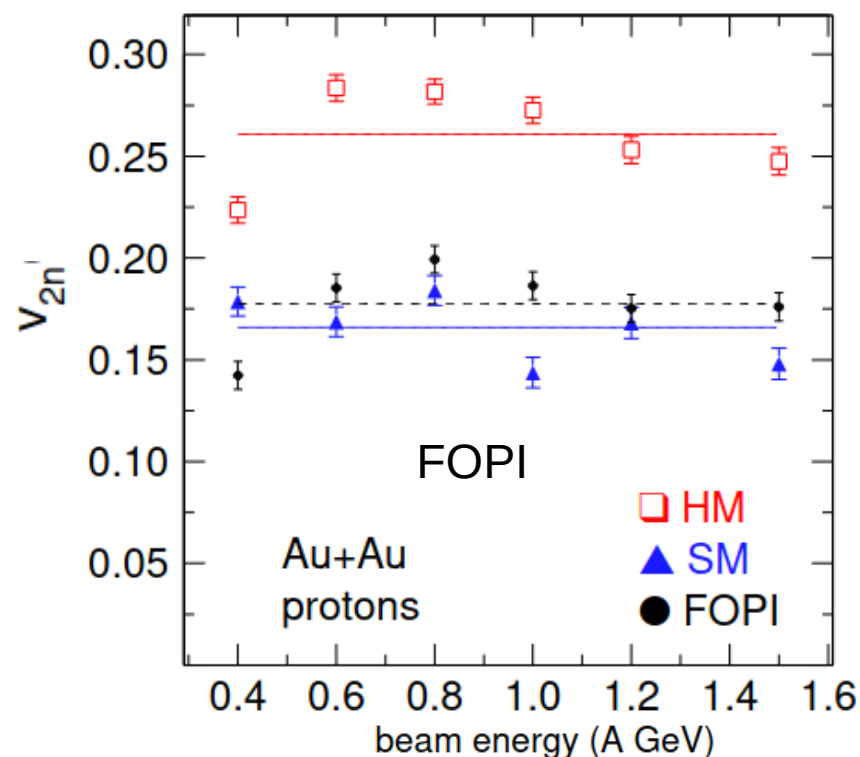
extensive database of experimental data for nucleonic observables for intermediate energy HIC (FOPI, HADES, S π RIT, KaOS and others)

have not been used to their full potential

approach similar to that of Danielewicz et al. (Science 298, 2002), potential residual biases avoided by simultaneously determining in-medium cross-sections, optical potential and EoS



Danielewicz et al., Science 298, 1592 (2002)



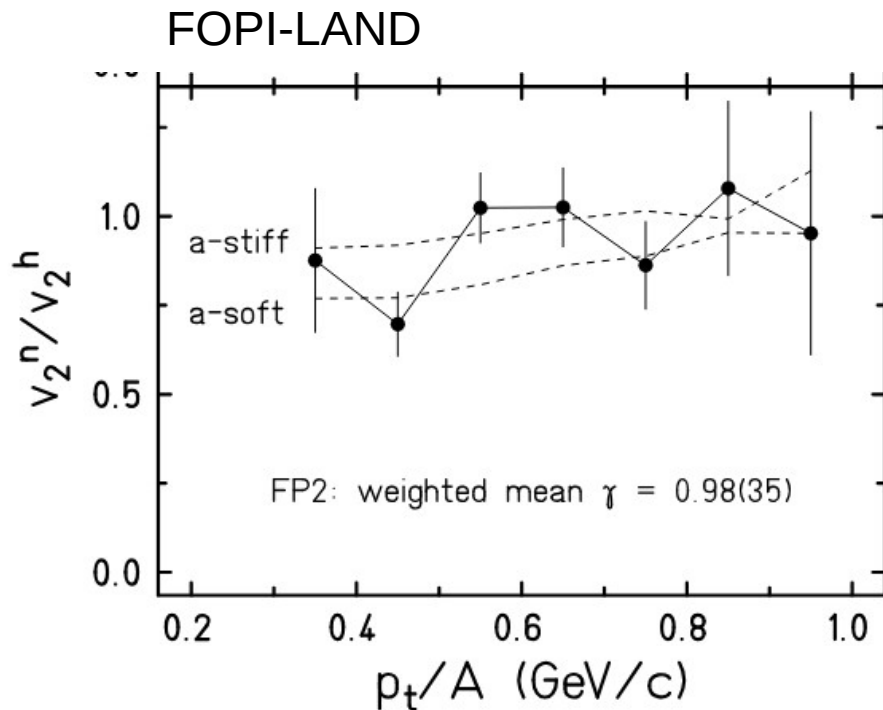
Le Fevre et al., NPA 945, 112 (2016)

Nucleonic Observables

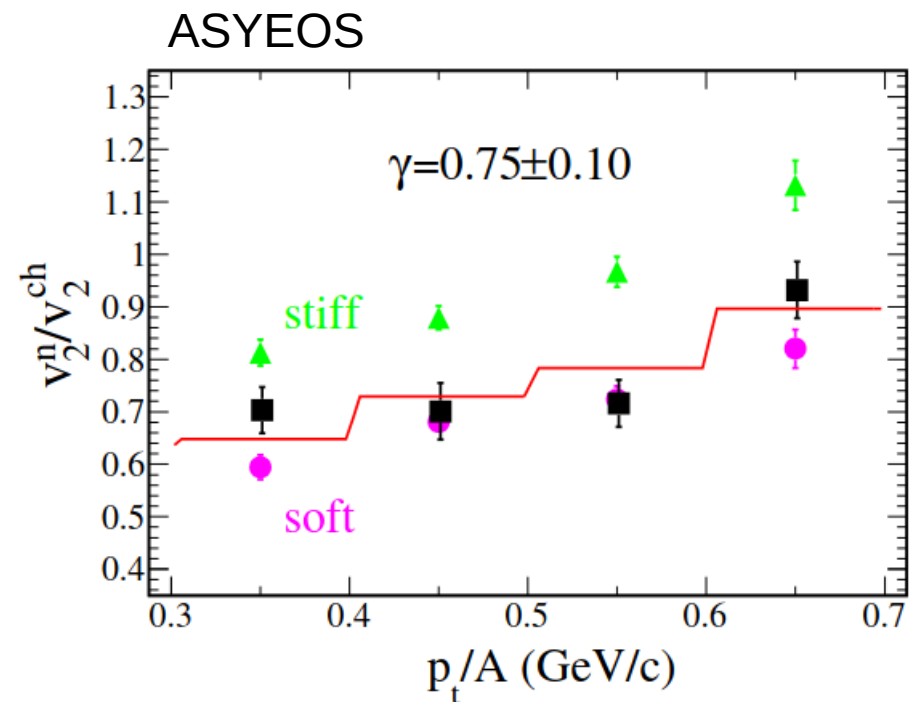
extensive database of experimental data for nucleonic observables for intermediate energy HIC (FOPI, HADES, S π RIT, KaOS and others)

have not been used to their full potential

approach similar to that of Danielewicz et al. (Science 298, 2002), potential biases avoided by simultaneously determining in-medium cross-sections, optical potential and EoS



P. Russotto et al., PLB 697, 471 (2011)



P. Russotto et al., PRC 94, 034608 (2016)

S π RIT Collaboration: C.Y.Tsang et al. PLB 853, 138661 (2024) (see also talks of M.Kurata-Nishimura, B. Tsang)

Model Details

dcQMD transport model: newest versions [EPJA 57, 309 \(2021\)](#)
[arXiv:2407.16411](#)

an upgraded version of TuQMD, see H. Wolter et al.

[Prog.Part.Nucl.Phys. 125, 103962 \(2022\)](#)

Interaction (nucleonic component)

momentum dependent potential **MDI2**

-generalization of MDI of

$$\frac{E}{N}(\rho, \beta, \mathbf{x}, \mathbf{y}) = \frac{1}{2} A_1 u + \frac{1}{2} A_2(\mathbf{x}, \mathbf{y}) u \beta^2 + \frac{B u^\sigma}{\sigma+1} (1 - \mathbf{x} \beta^2) + \frac{D u^2}{3} (1 - \mathbf{y} \beta^2)$$

Das, Das Gupta, Gale, Li PRC67, 034611 (2003)

$$A_2(\mathbf{x}, \mathbf{y}) = A_2^0 + \frac{2 \mathbf{x} B}{\sigma+1} \bar{u}^{\sigma-1} + \frac{2 \mathbf{y} D}{3} \bar{u}$$

$$u = \frac{\rho}{\rho_0}$$

Fit:

U_∞, K_0, J_0, m^* -isoscalar

$S(\tilde{u}), L, K_{\text{sym}}, \delta m_{\text{isv}}$ -isovector

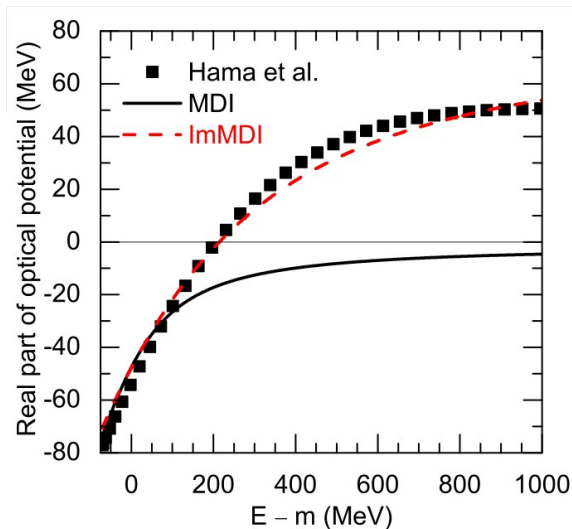
momentum dependent part: similar with that of J. Xu et al. PRC 91, 014611 (2015)

(see also C. Hartnack, J. Aichelin PRC 49, 2801 (1994))

used previously to test model dependence: flow ratio PRC 88, 44912 (2013)

pion multiplicity ratio PLB 753, 166 (2016)

independent part: extra term (vary L vs. K_{sym} and also J_0 vs. K independently)



from J. Xu et al. PRC 91, 014611 (2015)

Input		Parameters	
ρ_0 [fm^{-3}]	0.16	A [MeV]	708.001
E_B [MeV]	-16.0	C_l [MeV]	-13.183
m_s^*/m	0.70	C_u [MeV]	-140.405
δ_{n-p}^* ($\rho_0, \beta = 0.5$)	0.165	B [MeV]	137.305
K_0 [MeV]	245.0	σ	1.2516
J_0 [MeV]	-350.0	\tilde{A}_l [MeV]	-130.495
$\tilde{\rho}$ [fm^{-3}]	0.10	\tilde{A}_u [MeV]	-8.828
$S(\tilde{\rho})$ [MeV]	25.4	D [MeV]	7.357

Threshold Effects (dcQMD)

- **direct consequence** of imposing (total) energy conservation in the medium

$$\sqrt{p_1^2 + m_1^2} + U(p_1) + \sqrt{p_2^2 + m_2^2} + U(p_2) = \sqrt{p_1'^2 + m_1'^2} + U(p_1') + \sqrt{p_2'^2 + m_2'^2} + U(p_2')$$

- **only few** transport models below 1 AGeV:

RBUU: G. Ferini et al. PRL 97, 202301 (2006), RVUU: T. Song, C.M. Ko PRC 91, 014901 (2015);
 χ BUU: Z. Zhang et al, PRC 98, 054614 (2018), AMD+JAM: N. Ikeno et al., PRC 108, 044601 (2023)

- **required** for thermodynamical consistency of the model

Z.Zhang et al, PRC 97, 014610 (2018)

- **reactions:** NN \leftrightarrow NN, NN \leftrightarrow NR, R \leftrightarrow N π (R \leftrightarrow N $\pi\pi$ not corrected)

- **assumptions** (dcQMD): - two-body collisions are part of N-body one

- in-medium two-body collisions modeled as a succession of bare (vacuum-like) collisions followed/preceded by energy exchanges with the fireball, while momentum is conserved
- reaction with highest probability: corresponds to the one which included the bare collision of highest probability

Example: elastic NN

$$\frac{d\sigma^{(med)}}{d\Omega} = (2\pi)^4 \frac{m_1^* m_2^*}{k_i^* \sqrt{s_i^*}} |M_{fi}^{(med)}(\rho, \delta, \{\tau\})|^2 \frac{k_f^* m_1^* m_2^*}{\sqrt{s_f^*}}$$

$$|M_{fi}^{(med)}(\rho, \delta, \{\tau\})|^2 = \frac{1}{2} (|M_{fi}^{(vac)}(\tilde{s}_i)|^2 + |M_{fi}^{(vac)}(\tilde{s}_f)|^2) \longleftarrow \sqrt{\tilde{s}_{i,f}} - 2m_N = \sqrt{s_{i,f}^*} - \sqrt{s_{th}^*} + U_{i,f} - U_{th}$$

Introduced in TuQMD/dcQMD in [DC, PLB 753, 166 \(2016\)](#)

Collision Term

Elastic baryon-baryon collisions

-modified Cugnon parametrization to accurately describe elastic cross-sections at low impact energy (<100 MeV) but also total cross-sections above pion production threshold

J. Cugnon et al., NIMB 111, 215 (1996)

In-medium modification factor

- collision criterion based on effective masses determined using EoS (consistency with the $dt \rightarrow 0$ fm/c limit)
- in-medium modification of elastic cross-sections

$$\sigma^{med} = f(\rho, \delta) \sigma_{mod}^{vac}$$

$$f(\rho, \delta) = \exp[\alpha \rho / \rho_0 + \beta_1 \delta \rho / \rho_0 + \beta_2 (\tau_1 + \tau_2) \delta \rho / \rho_0]$$

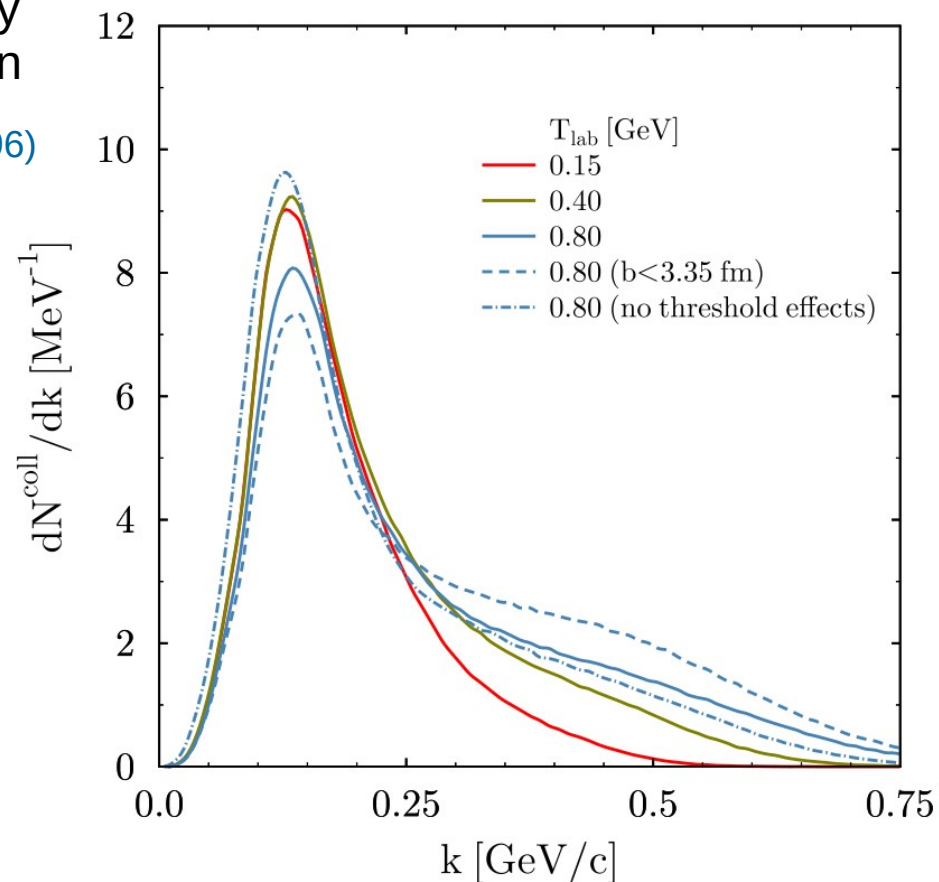
σ_{mod}^{vac} – flux and phase-space factors
computed using effective masses

B.A. Li et al. PRC72, 064611 (2005)

$f(\rho, \delta)$ – accounts for medium modifications of transition matrix due to departure from the quasi-particle picture

C. Fuchs et al. PRC 64, 024003 (2001)

Isospin dependent Pauli blocking (including a modified surface term)

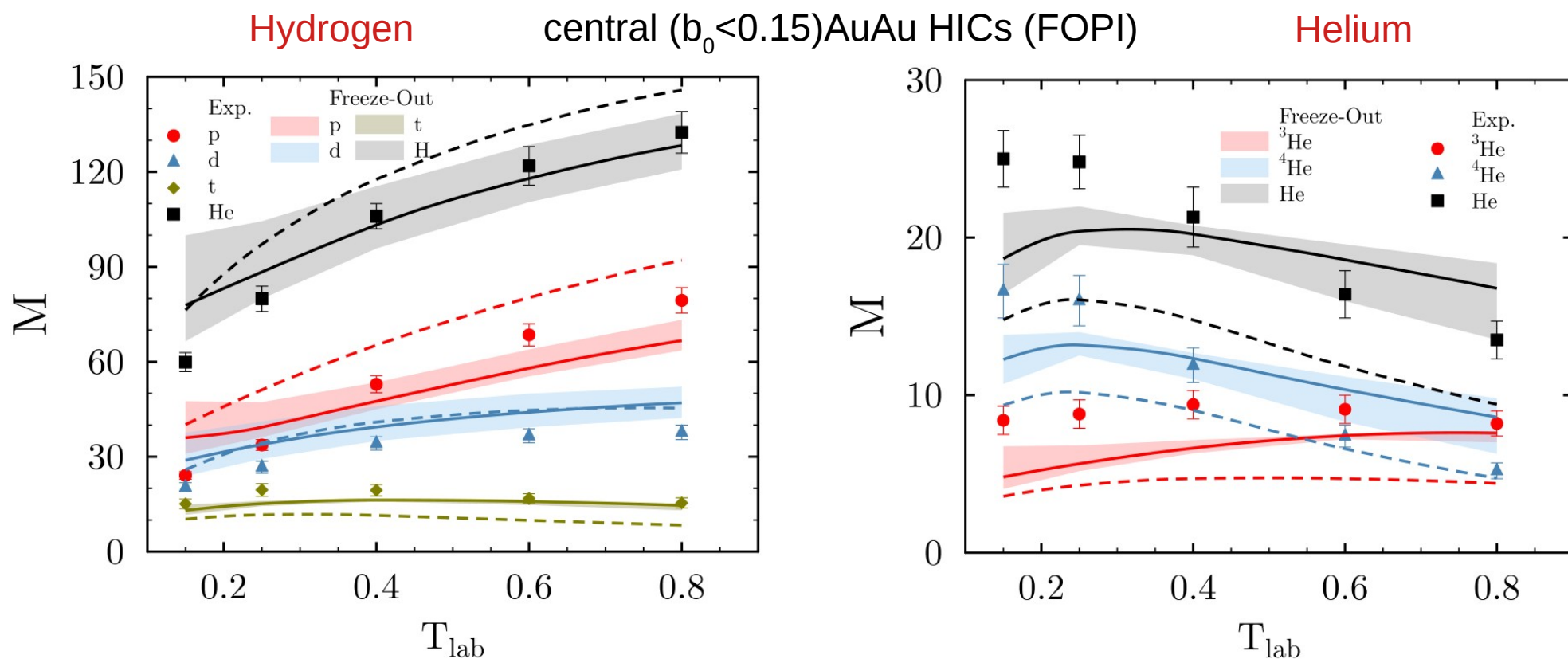


Resonance production: OBE model

S.Huber et al., NPA 573, 587 (1994)

Cluster multiplicities

- **final state:** MST algorithm all stable clusters ($\tau > 1\text{ms}$) with $A \leq 15$, 23 additional $A > 15$ (B,C,N,O)
- coalescence algorithm applied at **local freeze-out time**
- transport model parameters determined from a fit of v_1, v_2 and $\text{var}x_z$ experimental data
- $\delta r = 3.0\text{-}4.0\text{ fm}$, $\delta p = 0.2\text{-}0.3\text{ GeV}/c$



dashed curves: results with the coalescence model applied at final time (150 fm/c)

Nucleonic Observables

1) FOPI data set

- theoretical flow data away from mid-rapidity plagued by contamination from heavier clusters (most visible for proton $v_1(p_T)$ but also $v_1(y)$)
- exp data up 0.8 GeV/nucleon (impact of nucleon resonances on dynamics is small)

Label	Observables	Reference
FOPI1	$v_1(y)$, $ y \leq 0.5$ for $Z=1,2$ clusters; M5 centrality $^{197}\text{Au}+^{197}\text{Au}, ^{129}\text{Xe}+\text{CsI}, ^{58}\text{Ni}+^{58}\text{Ni}$ (0.25, 0.40)	A. Andronic et al. PRC 67, 034907(2003)
FOPI2	$v_1(y)$, $ y \leq 0.5$ for p, d, $A=3$ and α clusters; $0.25 \leq b_0 \leq 0.45$ $^{197}\text{Au}+^{197}\text{Au}$ (0.25, 0.40, 0.60, 0.80) $v_2(y)$, $ y \leq 0.5$ for p, d and α clusters; $0.25 \leq b_0 \leq 0.45$ $^{197}\text{Au}+^{197}\text{Au}$ (0.15, 0.25, 0.40, 0.60, 0.80) $v_2(p_T)$, $ y \leq 0.4$ for p, d and t clusters; $0.25 \leq b_0 \leq 0.45$ $^{197}\text{Au}+^{197}\text{Au}$ (0.15, 0.25, 0.40, 0.60, 0.80)	W. Reisdorf et al. NPA 876, 1 (2012)
varxz	varxz for p,d,t clusters; $b_0 \leq 0.15$ $^{40}\text{Ca}+^{40}\text{Ca}$ (0.4, 1.0), $^{58}\text{Ni}+^{58}\text{Ni}$ (0.15, 0.25), $^{96}\text{Ru}+^{96}\text{Ru}$ (0.4, 1.0) $^{96}\text{Zr}+^{96}\text{Zr}$ (0.4), $^{129}\text{Xe}+\text{CsI}$ (0.15, 0.25) $^{197}\text{Au}+^{197}\text{Au}$ (0.15, 0.25, 0.4, 0.6, 0.8)	W. Reisdorf et al. NPA 848, 366 (2010)
spectra	longitudinal and transverse rapidity spectra for protons in $Z \leq 3$ clusters $^{40}\text{Ca}+^{40}\text{Ca}$ (0.4), $b_0 \leq 0.15$, $ y_{L,T}/y_P \leq 1.25$	W. Reisdorf et al. PRL 92, 232301 (2004)

results using above data set only: [D.C. arXiv: 2407.16411](https://arxiv.org/abs/2407.16411)

Nucleonic Observables

- 2) FOPI-LAND, ASYEOS – dedicated symmetry energy measurement
- 3) SPIRIT – dedicated effective masses and symmetry energy campaign

Label	Observables	Reference
FOPI-LAND	$v_2(p_T)$, $0.25 \leq y \leq 0.75$ for $n, Z=1$; $b \leq 7.5$ fm $^{197}\text{Au}+^{197}\text{Au}$ (0.40)	P. Russotto et al. PLB 697, 471 (2011)
ASYEOS	$v_2(p_T)$, $0.3 \leq y \leq 0.7$ for $n, Z>0$; $b \leq 7.5$ fm $^{197}\text{Au}+^{197}\text{Au}$ (0.40)	P. Russotto et al. PRC 94, 034608 (2016)
SPIRIT	varxz for p,d,t clusters; $b \leq 1.6$ fm $^{112}\text{Sn}+^{124}\text{Sn}$ (0.27) $v_1(p_T), v_1(y), v_2(y)$ for p in $Z=1,2$ clusters; $3.6 \leq b \leq 6.3$ fm $^{132}\text{Sn}+^{124}\text{Sn}$ (0.27) $v_1(p_T), v_1(y), v_2(y)$ for p in $Z=1,2$ clusters; $4.0 \leq b \leq 6.0$ fm $^{108}\text{Sn}+^{112}\text{Sn}$ (0.27)	C.Y. Tsang et al. PLB 853, 138661 (2024)

Theoretical Simulations

Model parameters:

m^*	[0.6, 0.9]	isoscalar effective mass
V_∞	[25, 125] MeV	isoscalar potential $p \rightarrow \infty$
K_0	[165, 355] MeV	compressibility modulus
α	[-0.4, 0.8]	in-medium σ_{NN} , $\delta=0.0$
Δm_{np}^*	[-0.25,0.25] at $(\rho=\rho_0, \delta=0.5)$	n-p effective mass diff.
L	[15, 145] MeV	slope symmetry energy
β_1	[-0.5,3.5]	in-medium σ_{NN} , $\delta \neq 0.0$
β_2	[-1.5, 2.5]	$\sigma_{nn} \neq \sigma_{pp}$, $\delta \neq 0.0$

Enforced correlations:

$$J_0 = -600 + (K_0 - 165) * 3.125$$

$$K_{sym} = -488 + L * 6.728$$

in units of [MeV]

Input:

$$E/N(\rho_0) = -16.0 \text{ MeV}$$

$$S(0.62\rho_0) = 25.5 \text{ MeV}$$

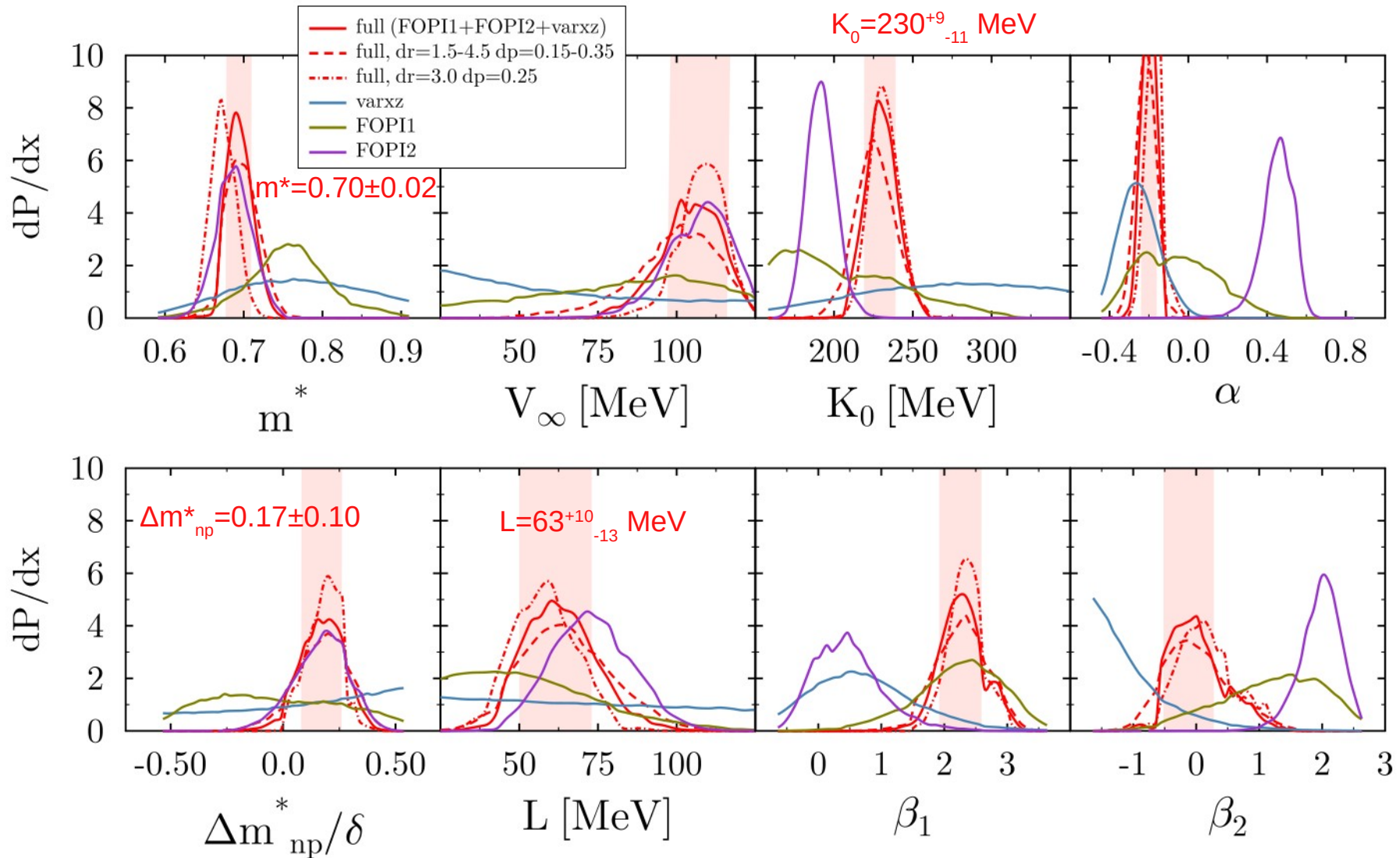
properties of doubly-magic nuclei
(binding energies, rms charge radii,
single particle energies)

Brown, PRL 111, 232502 (2013)

Model uncertainty: statistical+ systematical ($\delta r=3.0-4.0$ fm, $\delta p=0.2-0.3$ GeV/c)
added in quadrature

Model emulator: sum of monomials of degree ≤ 2 ; checked robustness LOO-CV method

Constraints

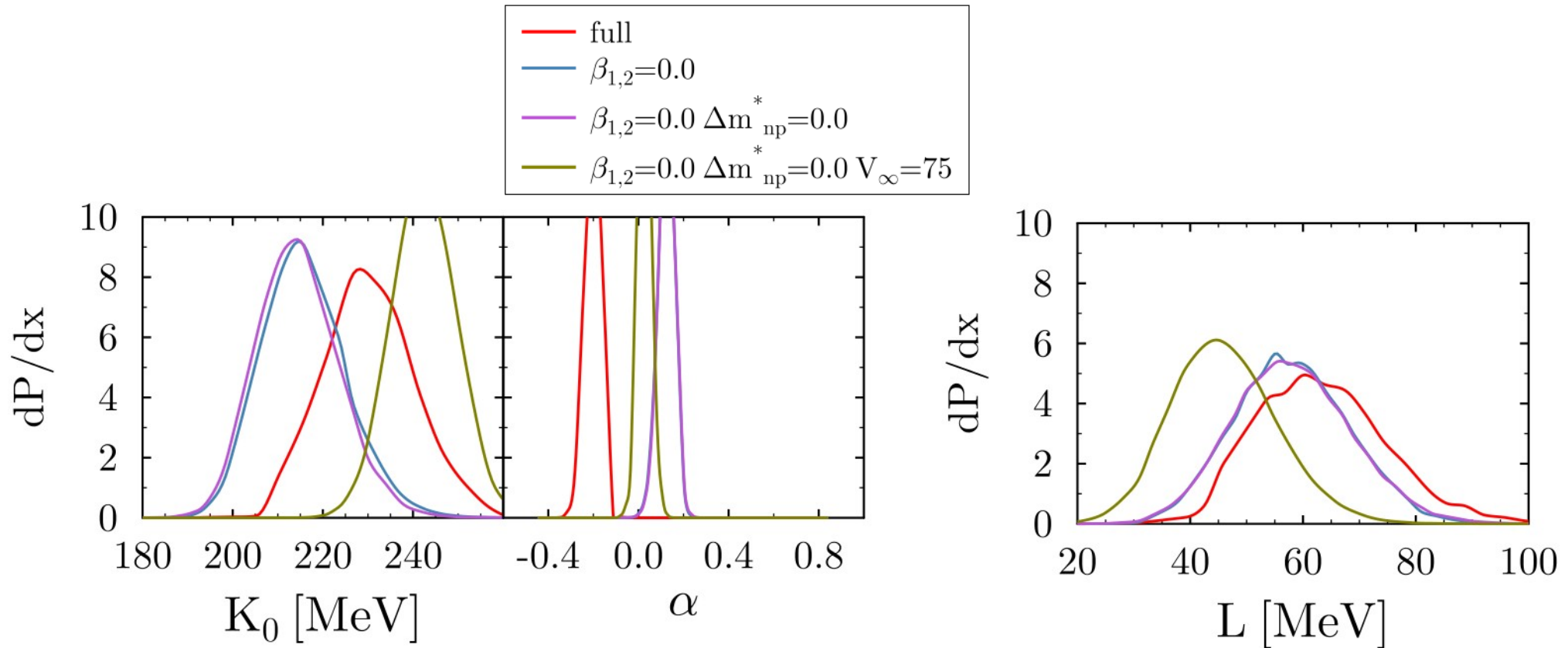


- exp data for isospin symmetric systems crucial for breaking degeneracy of isospin dep. and isospin indep. in-medium effects on cross-sections

Isospin asymmetry dependent σ_{NN}

$$\sigma^{med} = f(\rho, \delta) \sigma_{mod}^{vac}$$

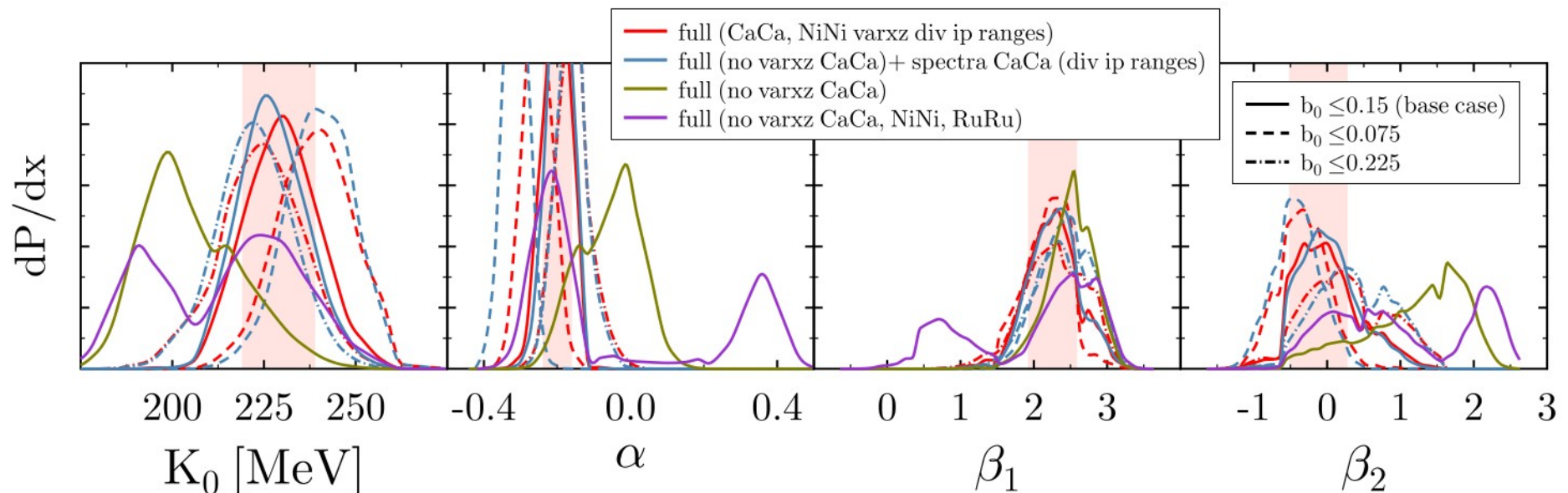
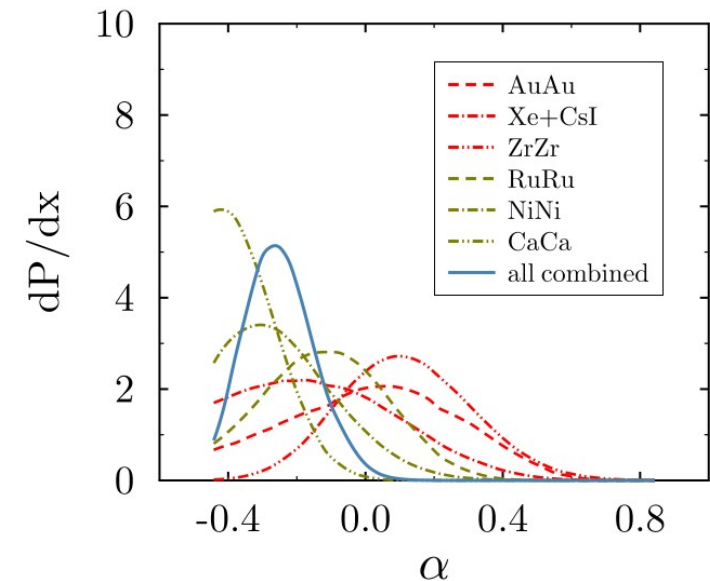
$f(\rho, \delta) = \exp[\alpha \rho / \rho_0 + \beta_1 \delta \rho / \rho_0 + \beta_2 (\tau_1 + \tau_2) \delta \rho / \rho_0]$ ← in-medium modification of the transition amplitude



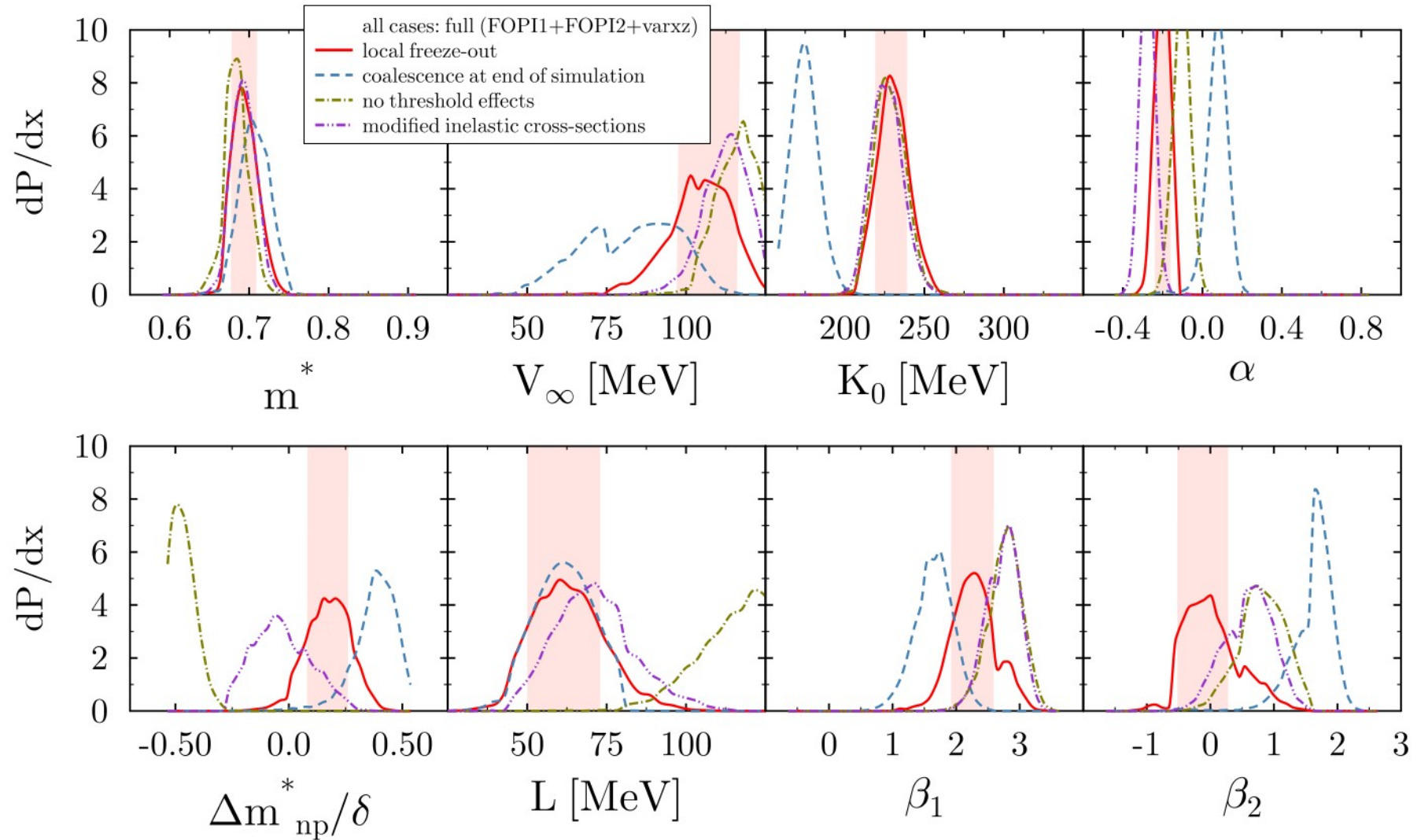
- setting $\Delta m_{np}^* = -0.5\delta$ leads to an impact on isoscalar m^* at 1σ level

Relevance of Isospin Symmetric Systems

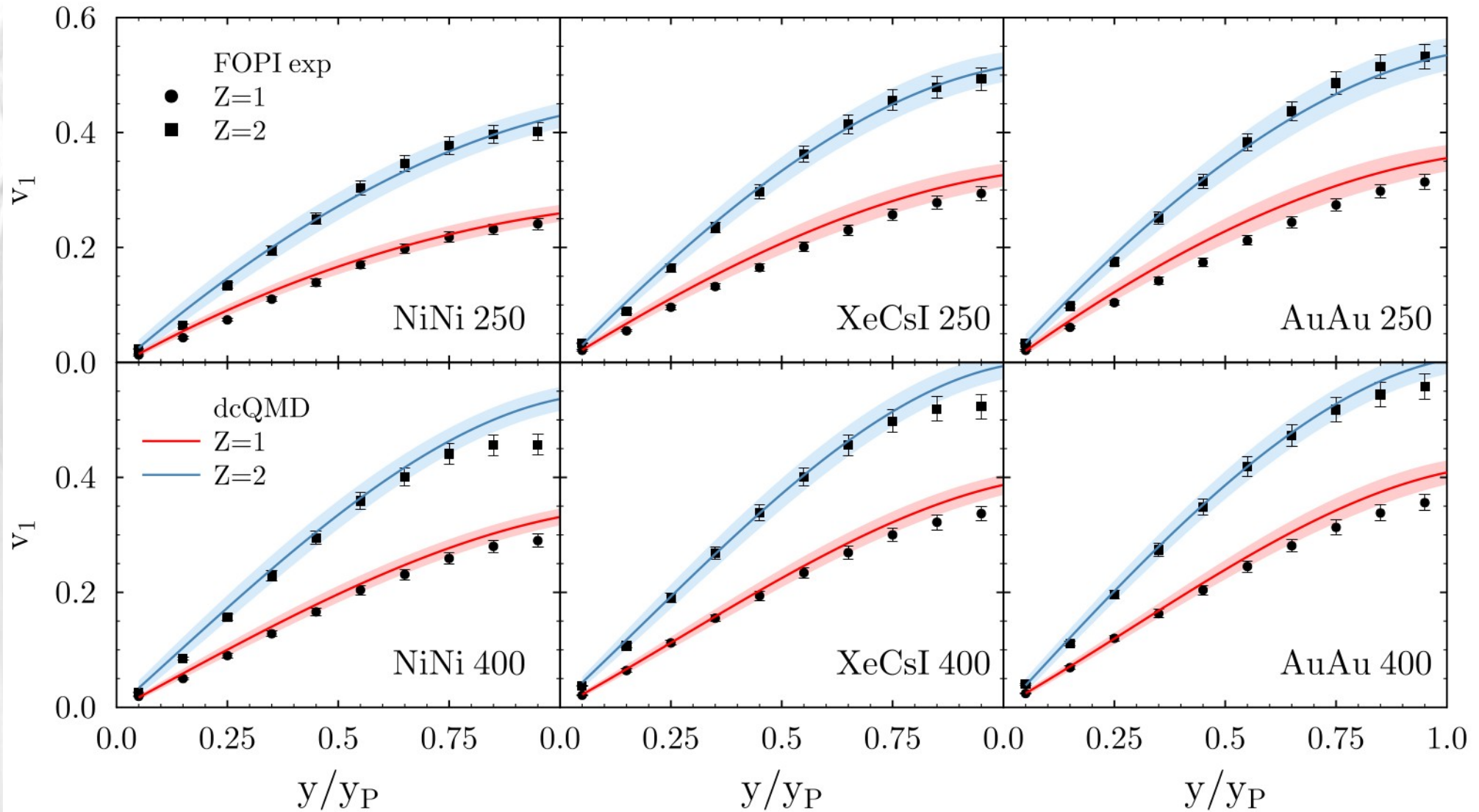
- isospin symmetric systems favor stronger in-medium reduction of cross-sections
- Pauli blocking algorithm less efficient for light system (~92% for AuAu vs. ~85% for CaCa)
- observed extra reduction ~25%
- $Z=1,2 v_1$ for NiNi crucial in breaking degeneracy between α and β_1



Threshold Effect and Inelastic Channels



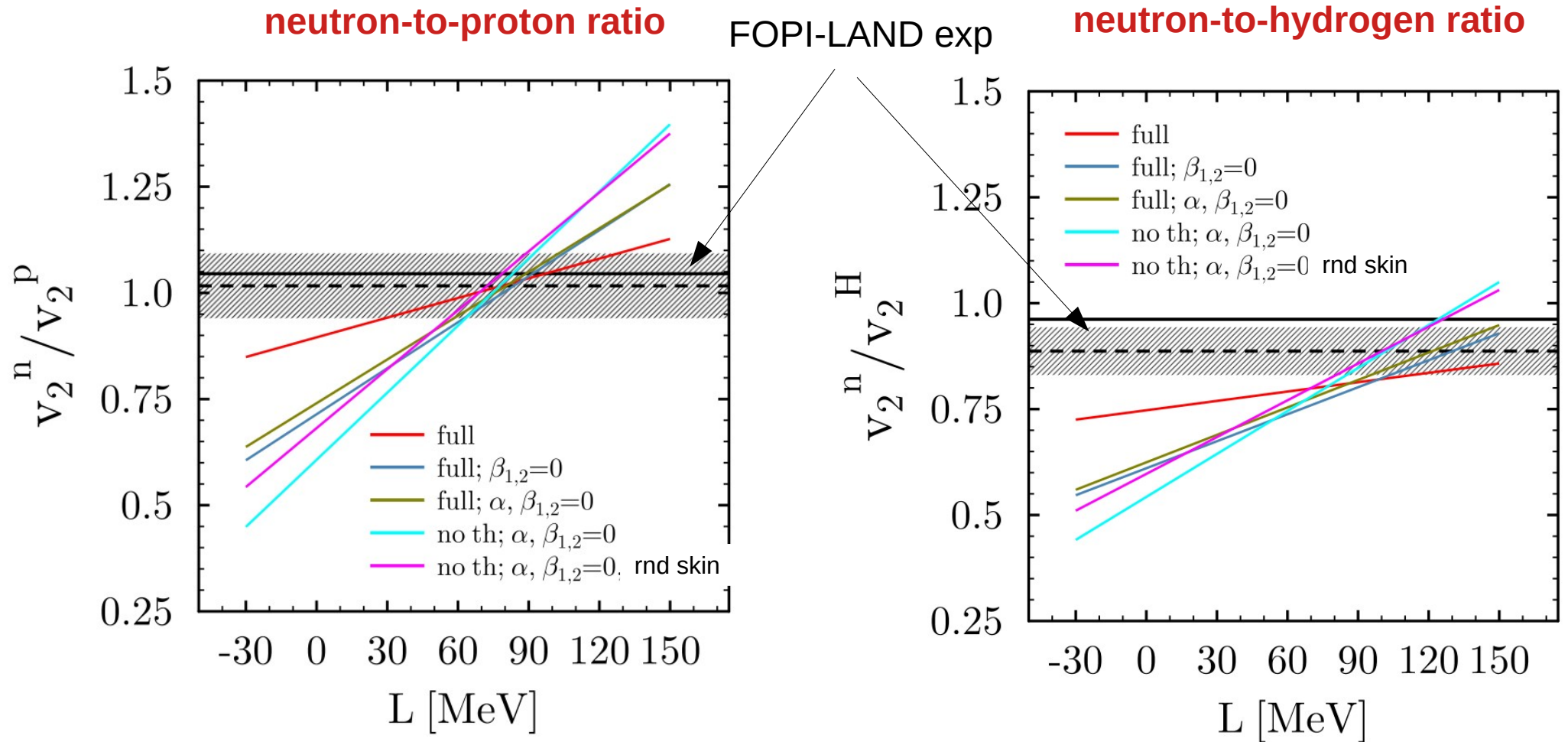
FOPI1: $v_1(y)$



- M5 centrality
- only data with $y/y_P < 0.5$ included in the fit

Full comparison to experimental data set:
see D.C. [arXiv:2407.16411](https://arxiv.org/abs/2407.16411)

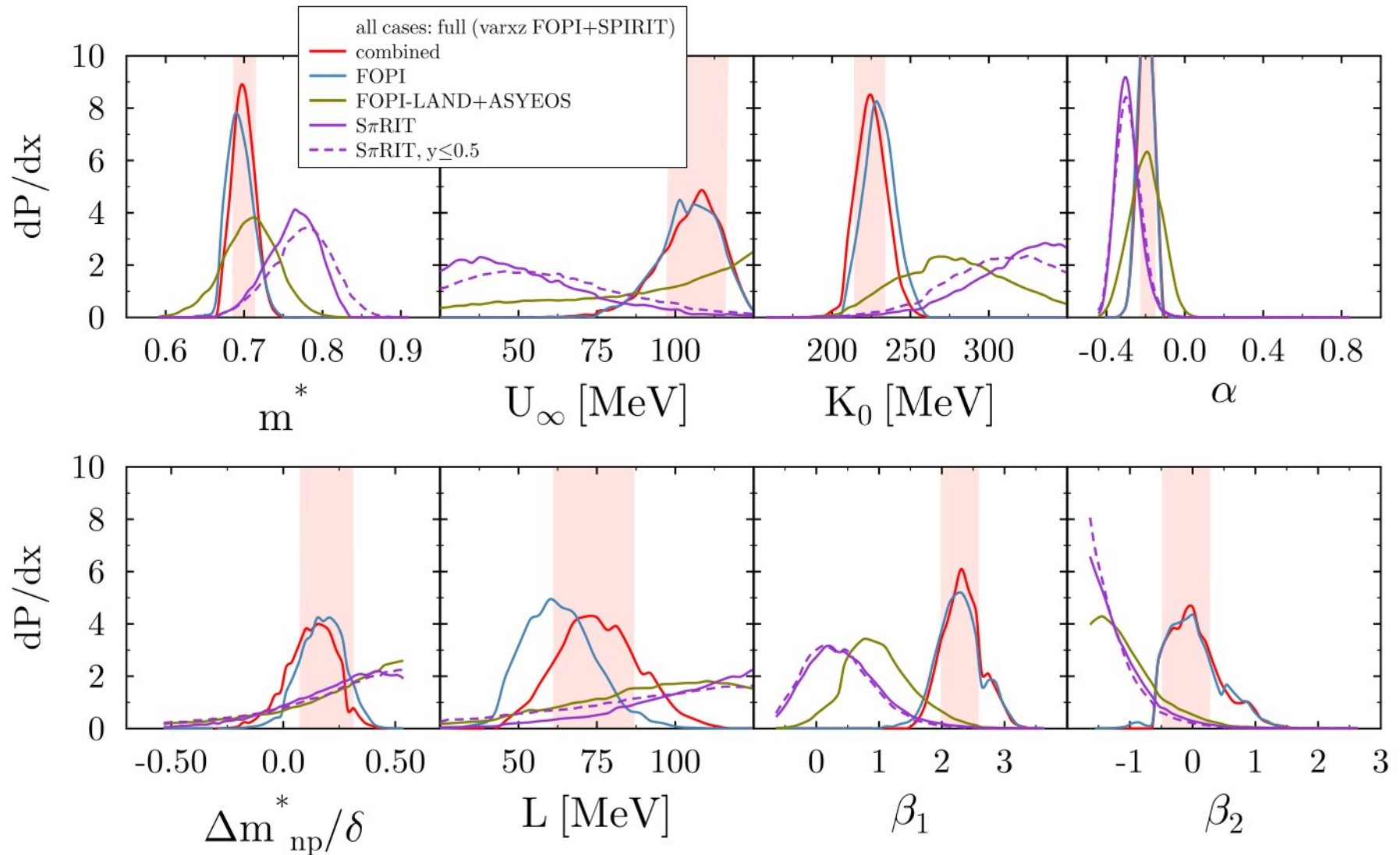
FOPI-LAND Experiment Revisited



- identical results for neutron-to-charged particles ratio (ASYEOS experiment)

- future ASYEOS2 measurement (2025) aims at determining n/p with greater accuracy

Combined Constraint

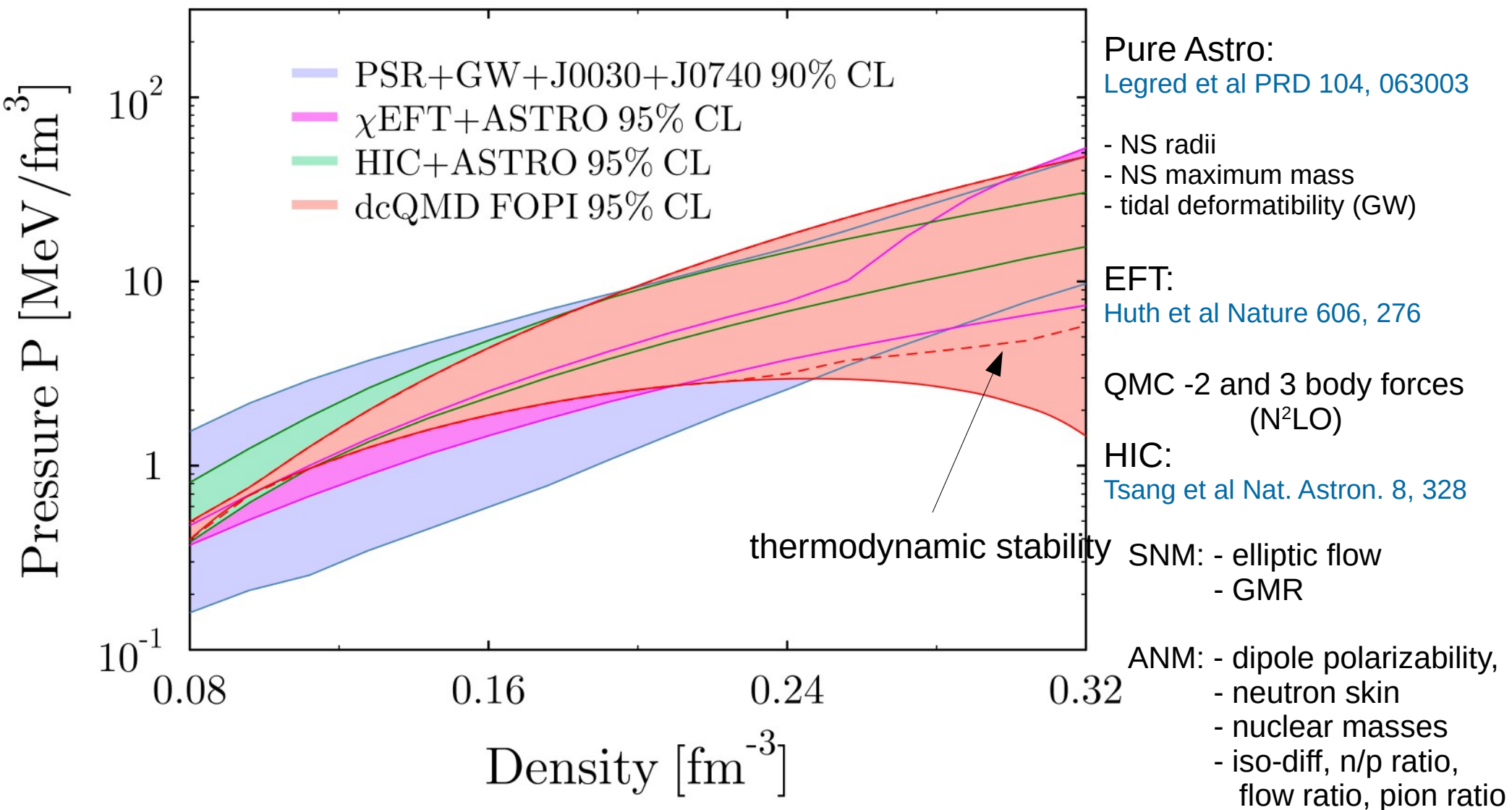


	FOPI	combined
K_0 [MeV]	230 ± 10	225 ± 10
L [MeV]	63 ± 10	74 ± 13

Pressure

Neutron star matter ($\delta=0.93$)

Input: $S(0.62\rho_0)=25.5$ MeV



Probed densities: see D.C. [arXiv:2407.16411](https://arxiv.org/abs/2407.16411)

Perspectives

Experimental side: ASYEOS (2025) v_2^n/v_2^p : AuAu 0.25, 0.40, 0.80 GeV/nucleon

HADES (2025?) nucleonic flows, pions: AuAu 0.40, 0.60, 0.80 GeV/nucleon

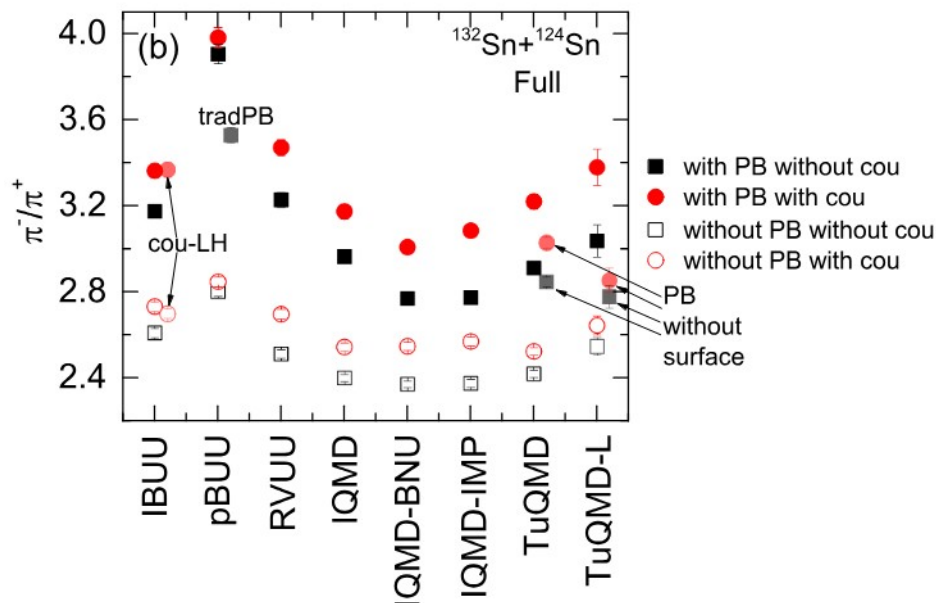
SπRIT (2024): nucleonic, pionic observables Xe+Sn 0.34 GeV/nucleon

Theoretical side: - make use of lower p_T part of pion spectra (SπRIT): non-resonant pion production channels

- access higher densities: FOPI and HADES data above 1 GeV/nucleon: treat two-pion production channels consistently

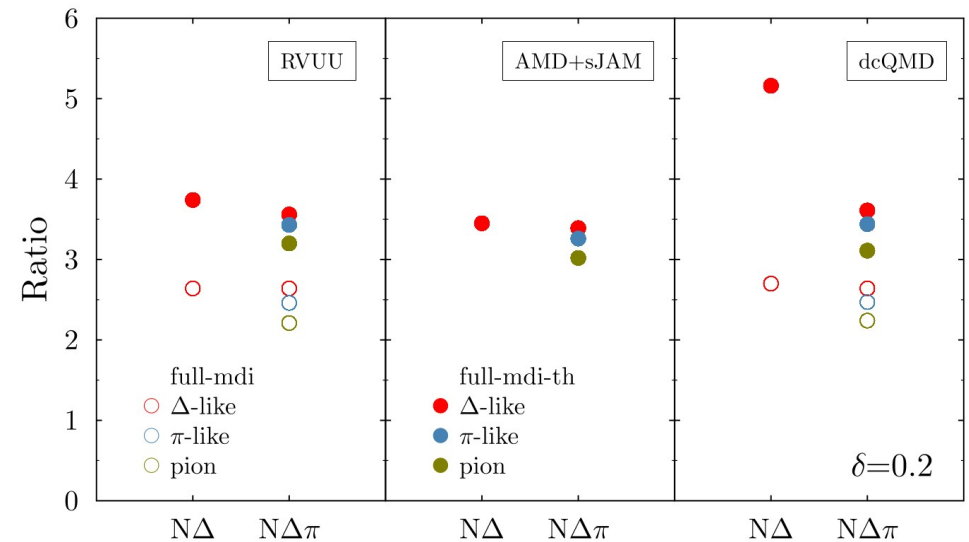
- assesment of systematic uncertainty of transport model predictions (TMEP)

HIC with MII



J. Xu et al. PRC 109, 044609 (2024)

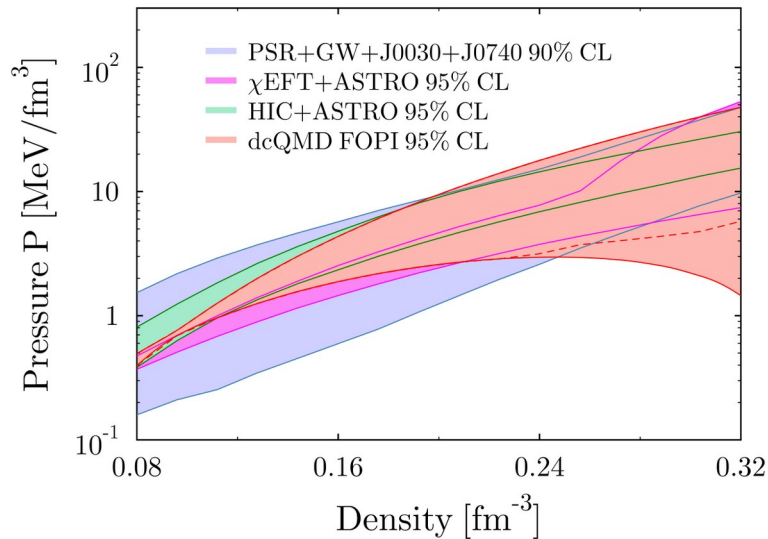
Collision integral with MDI in a box



D.C. et al. (TMEP), in preparation

Summary & Conclusions

Study of EoS, effective masses and σ^* using nucleonic observables in AuAu collisions of intermediate impact energy (0.15-0.80 GeV/nucleon)



68% CL Result

$$m^* = 0.70 \pm 0.02 \quad V_\infty = 104 \pm 8 \text{ MeV}$$

$$\Delta m_{np}^* = (0.17 \pm 0.10) \delta$$

$$K_0 = 230 \pm 10 \text{ MeV}$$

$$L = 63 \pm 12 \text{ MeV}$$

- in-medium effects on elastic collisions that depend on density, isospin asymmetry and isospin projection
- clusterization algorithm applied at local freeze-out time
- systematic uncertainty due to coalescence parameters;
- constraints extracted from FOPI experimental data for $v_1(y)$, $v_2(y)$, $v_2(p_T)$ and $\text{var}x_z$
- model dependence: threshold effects and isospin asymmetry dependence of σ^* have significant impact

Comparison to a study of SE using pionic observables

- full agreement (in contradiction with the situation ~10 years ago)

Perspectives: - remove imposed correlation between $L_0 \leftrightarrow J_0$ and $L \leftrightarrow K_{\text{sym}}$; allow for a variation of $E/N(\rho_0)$ and $S(0.1 \text{ fm}^{-3})$.

- include explicit cluster degrees of freedom to be able to use experimental data sets to their full potential
- improve model to use more accurate part of pion spectra and access higher densities with HIC above 1.0 GeV/nucleon
- estimate model dependence (TMEP)

Probed Density (Free Protons)

- observables are functionals of the EoS
- sensitivity: functional derivatives w.r.t to EoS or $d \text{ EoS} / d\rho$, etc.

$$\frac{d \text{ Obs}}{d \text{ EoS}} = \frac{\lim_{\epsilon \rightarrow 0} \text{Obs} \left[\frac{d \text{ EoS}}{d \rho}(\rho) + \epsilon \delta(\rho - \tilde{\rho}) \right] - \text{Obs} \left[\frac{d \text{ EoS}}{d \rho}(\rho) - \epsilon \delta(\rho - \tilde{\rho}) \right]}{2\epsilon}$$

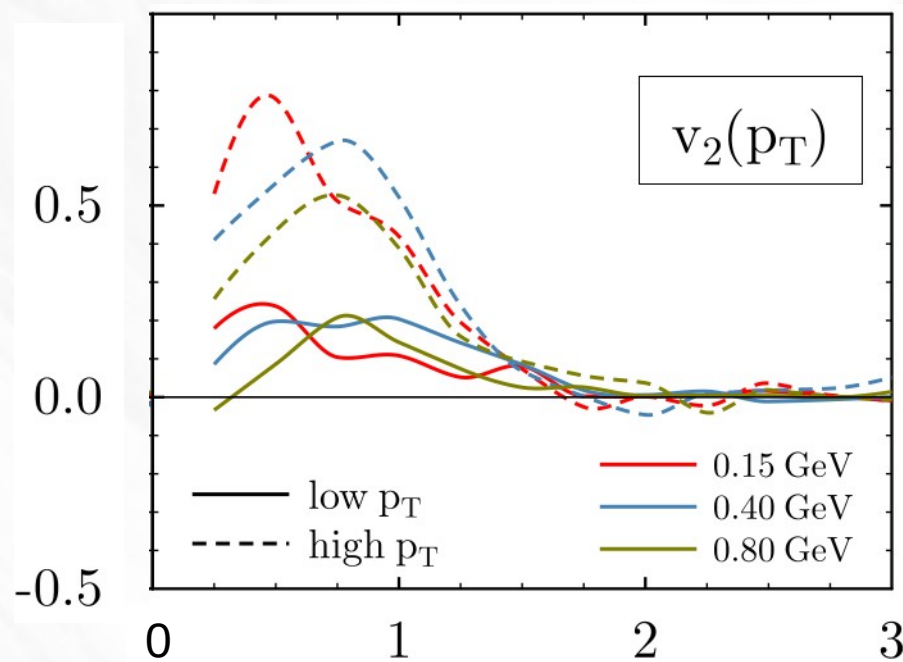
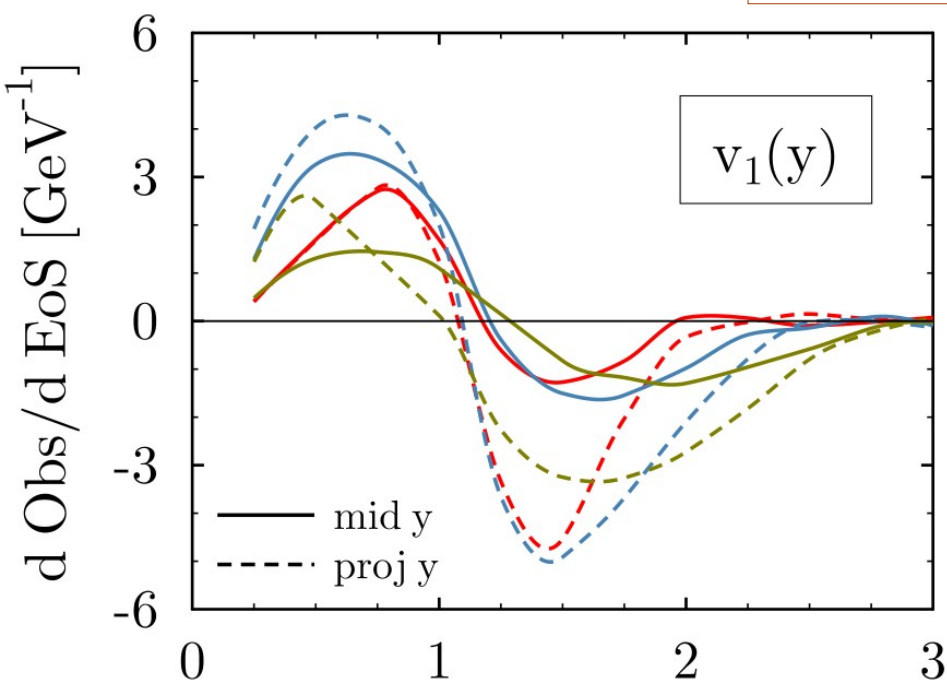
$$\Delta \langle H_{L_0} \rangle = \sum_{i=n,p} \frac{\epsilon}{2} \left[\text{Erf} \left(\frac{\tilde{u}}{\eta} \right) - \text{Erf} \left(\frac{\tilde{u} - u_i}{\eta} \right) \right] \quad (1)$$

$$\Delta \langle H_L \rangle = \sum_{i=n,p} \frac{\epsilon}{2} \tilde{\tau}_i \delta_i \left[\text{Erf} \left(\frac{\tilde{u}}{\eta} \right) - \text{Erf} \left(\frac{\tilde{u} - u_i}{\eta} \right) \right]$$

Isoscalar EoS

AuAu 3.35 < b < 6.0 fm

Symmetry Energy

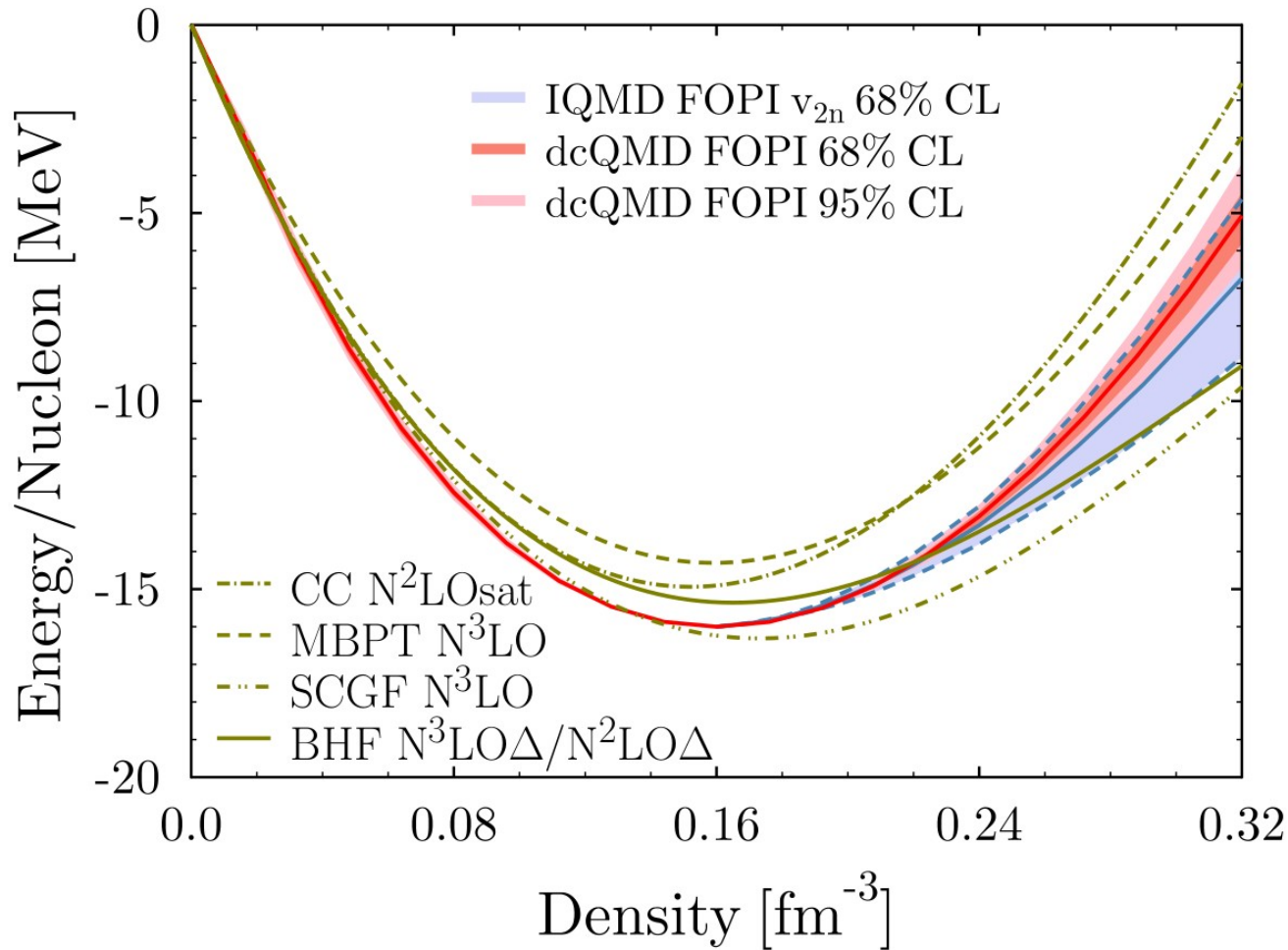


$\tilde{\rho} / \rho_0$
 mid y: $0.0 < y/y_p < 0.5$
 proj y: $0.5 < y/y_p < 1.0$

— 0.15 GeV
 — 0.40 GeV
 — 0.80 GeV

$\tilde{\rho} / \rho_0$
 low p_T : $0.4 < p_T/p_p < 1.2$
 high p_T : $1.2 < p_T/p_p < 2.0$

EoS of Symmetric Matter



$$K_0 = 230 \pm 10 \text{ MeV } 68\% \text{CL}$$

IQMD result:

A. Le Fevre et al., NPA 945, 112 (2016)

$$K_0 = 190 \pm 30 \text{ MeV } 68\% \text{CL}$$

Microscopic calculations:

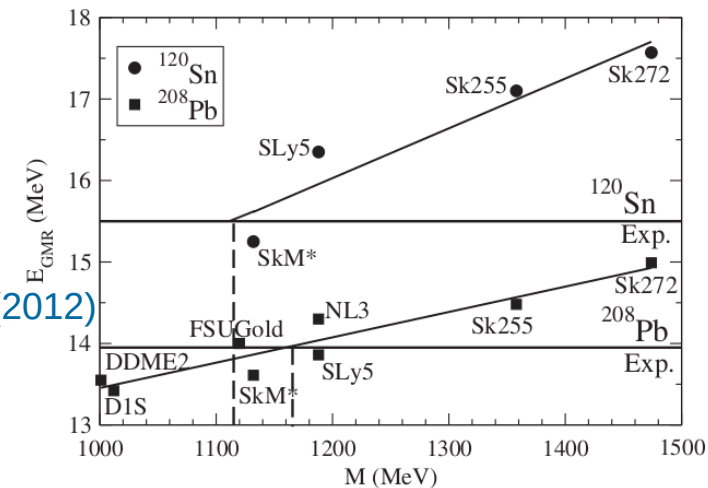
1. A. Ekstrom et al., PRC 91, 051301 (2015)
2. C. Drischler et al., PRC 102, 054315 (2020)
3. A. Carbone, PRR 2, 023227 (2020)
4. D. Logoteta, PRC 94, 064001 (2016)c

centroid of GMR correlated with derivative of incompressibility

$$M = 3\rho K'(\rho)|_{\rho=\rho_c} \quad \rho_c = 0.11 \text{ fm}^{-3} \quad \text{E.Khan et. al PRL 109, 092501 (2012)}$$

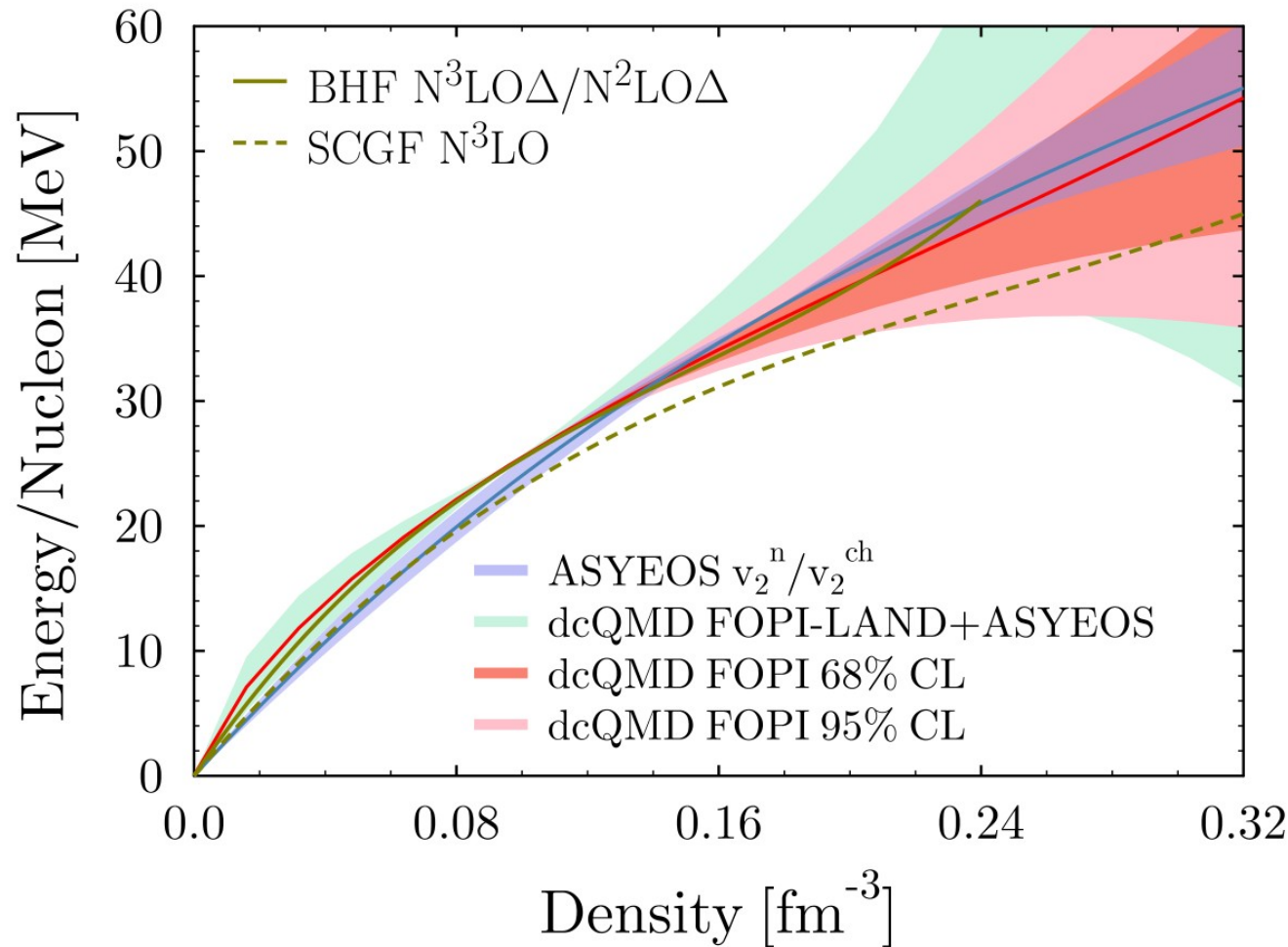
$$^{112-124}\text{Sn}, ^{208}\text{Pb}, ^{90}\text{Zr}, ^{144}\text{Sm} \rightarrow M = 1100 \pm 70 \text{ MeV}$$

this work: $M = 1110 \pm 40 \text{ MeV}$



Symmetry Energy

Input: $S(0.62\rho_0)=25.5$ MeV



$L=63 \pm 10$ MeV 68%CL
 $S(\rho_0)=34.3 \pm 1.1$ MeV
 $S(2\rho_0)=54.2 \pm 12.4$ MeV

ASYEOS result:

$L=72 \pm 13$ MeV 68%CL $S_0=34$ MeV

$L=63 \pm 11$ MeV 68%CL $S_0=31$ MeV

P. Russotto et al., PRC 94, 034608 (2016)

Microscopic calculations:

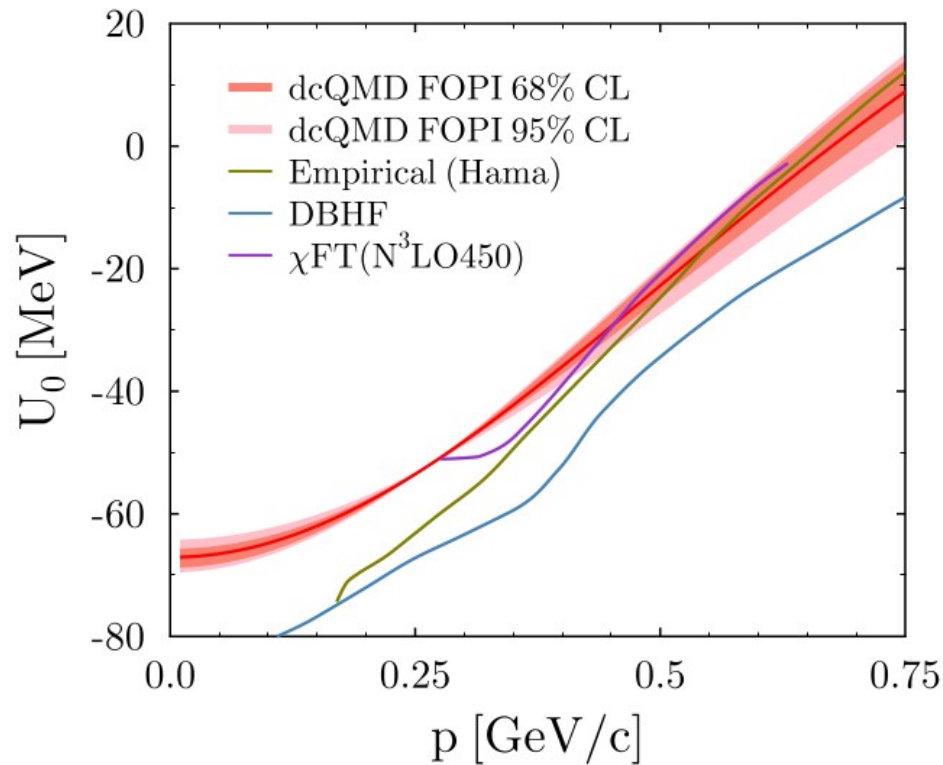
SCGF: A. Carbone, PRR 2, 023227 (2020)

BHF: D. Logoteta, PRC 94, 064001 (2016)c

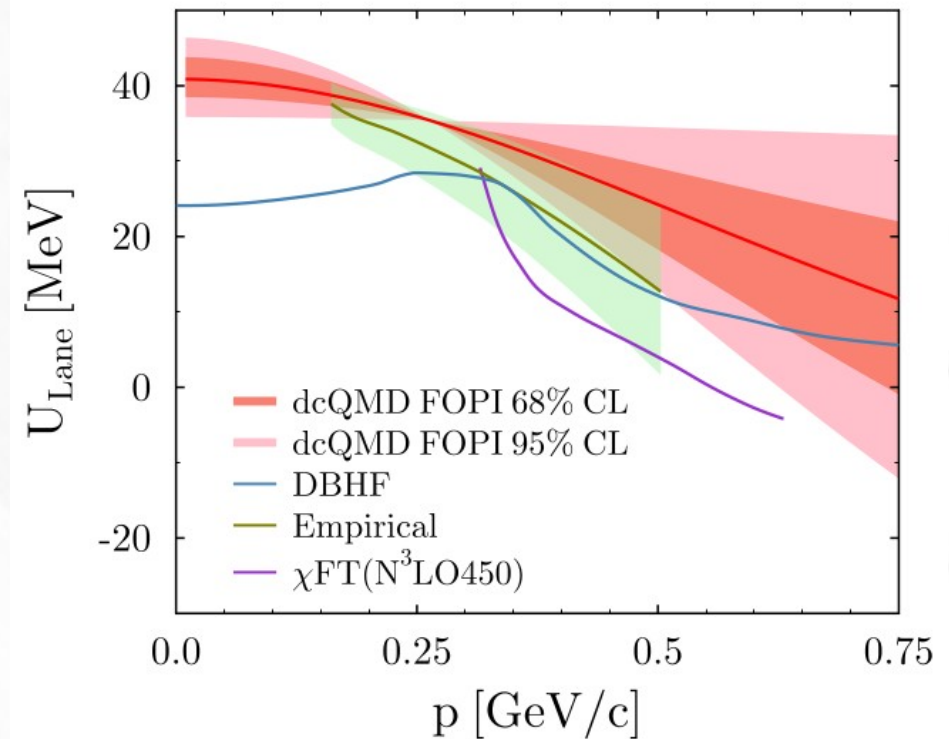
Momentum dependent optical potential

Isoscalar Potential

at saturation density



Lane Potential



DBHF: van Dalen et al., PRC 72, 065803 (2005)

Empirical Lane: B.A. Li, PRC 69, 064602 (2004)

χ FT: J.W. Holt et al., PRC 93, 064603 (2016)

In-medium σ_{NN} (T=0 MeV Fermi)

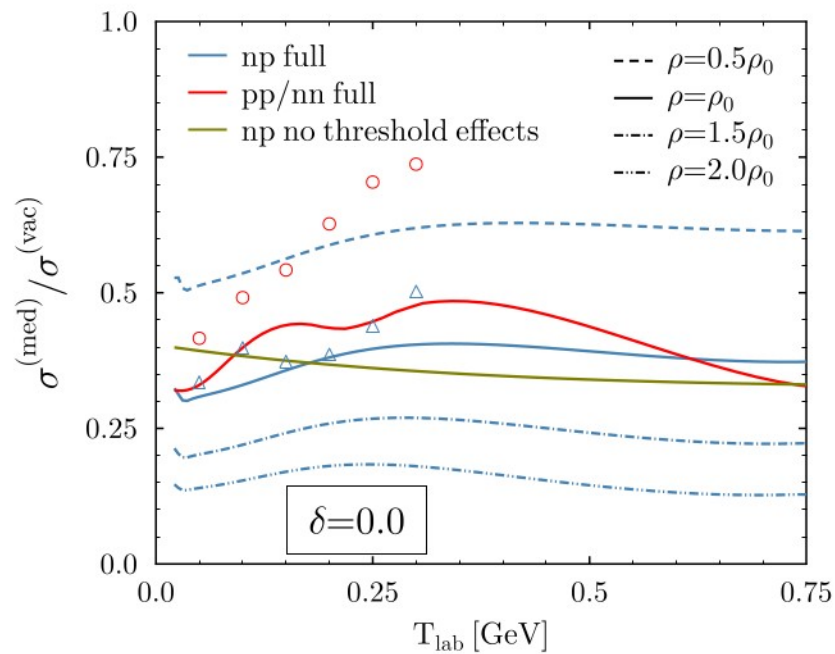
$$\frac{d\sigma^{(med)}}{d\Omega} = (2\pi)^4 \frac{m_1^* m_2^*}{k_i^* \sqrt{s_i^*}} |M_{fi}^{(med)}(\rho, \delta, \{\tau\})|^2 \frac{k_f^* m_1^* m_2^*}{\sqrt{s_f^*}}$$

$$|M_{fi}^{(med)}(\rho, \delta, \{\tau\})|^2 = \frac{1}{2} (|M_{fi}^{(vac)}(\tilde{s}_i)|^2 + |M_{fi}^{(vac)}(\tilde{s}_f)|^2) \leftarrow \sqrt{\tilde{s}_{i,f}} - 2m_N = \sqrt{s_{i,f}^*} - \sqrt{s_{th}^*} + U_{i,f} - U_{th}$$

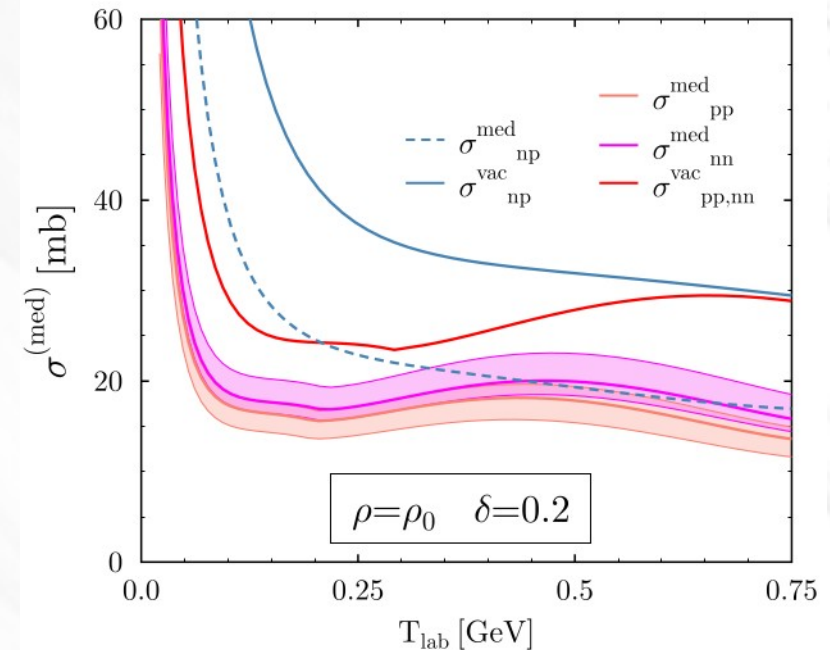
$$\times \exp [(\alpha + \beta_1 \delta + \beta_2 (\tau_1 + \tau_2) \delta) \frac{\rho}{\rho_0}]$$

reduction factor in symmetric matter

asymmetric nuclear matter



P=0.0



Li, Machleidt, PRC 48, 1702 (1993)
Li, Machleidt, PRC 49, 566 (1994)

qualitative agreement
with microscopical models

H. Zhang et al., IJMPE 19, 1788 (2010)
F. Sammarruca, EPJA 50, 22 (2014)